BRNO UNIVERSITY OF TECHNOLOGY

FACULTY OF MECHANICAL ENGINEERING

INSTITUTE OF MATERIAL SCIENCE AND ENGINEERING

Ing. Gianmarco Taveri

GEOPOLYMERS INCORPORATING WASTES AND COMPOSITES PROCESSING

Short version Ph. D. thesis

Field: Physical and Materials Engineering

Supervisor: Prof. Ing. Ivo Dlouhý, CSc.

Keywords

Geopolymers, polycondensation, composite materials, mechanical properties, fracture toughness, hydro-pressure sintering, spectroscopy.

Contents

1. Introduction

The construction industry encountered the primary needs and demand of the humankind since ever, not only supporting the realization and maintenance of any infrastructure and building, including safe dwells and living places, but also providing new ideas and technology for the future. It is well understood that since the ancient ages, the human was always looking for material aesthetically pleasant and in the same time practically performing and durable.
In addition, nowadays, the world is facing several environmental issues, including the global emergency of the climate change, a constant increase of the season average temperature, with the consecutive modification of the ecosystem, due to extensive emission in the atmosphere of greenhouse gasses, among all the carbon dioxide (CO_2), and the undue exploitation of open air landfills, as the disposal of trash of any nature is rapidly increasing. For instance, a sizeable share (around 8%) is covered by the production of the Portland cement (OPC), the most exploited material in the world for constructions and building engineering application [1,2]. Besides, the steady increase in the industrialization worldwide is yielding to a disposal of a huge annual amount of industrial wastes and slags, which can be rather reutilized for some other purposes [3].
Due to these reason, new materials for construction applications must encounter safety, durability and performance requirements, while its production should include zero greenhouse emissions and incorporation of wastes. One of the possible ways is to introduce in the market durable and eco-friendly materials like geopolymer (GP). The processing of this material is also compliant with the incorporation of recyclable wastes, like fly ash, a power plant by-product, and borosilicate glass, usually used for lab and pharmaceutical purposes [4]. In its applications, GPs are also versatile, including [5]:

- Construction and buildings
- Immobilization of toxic metals
- Refractory utilization

The utilization of compatible wastes in GPs, like fly ash (FA) and borosilicate glass (BSG), would adjust the chemistry of production, conferring mechanical performance, while reducing the cost of production. However, its brittleness and low resistance to crack propagation (fracture resistance) prompts the scientific community to look for some better solution. One of the ways is to produce composites made of fibers dispersed in the matrix. The extent of toughening depends on the type of fibers, their interaction with the matrix and their average size. Therefore, depending on what is meant to be obtained, several solutions are equally applicable. Incorporating cellulose fibers and recycled paper fibers in producing geopolymeric composites is one of compelling solutions to undertake [6,7]. Due to its specific tensile strength, cellulose fibers are expected to sensitively increase the mechanical properties and resistance to crack propagation of a geopolymeric matrix [8].

2. Scopes and aims of the thesis

Geopolymers incorporating aluminosilicate wastes was the baseline of the whole thesis work. The utilization of FA, a power plant by-product, and borosilicate glass, a recycled glass from pharmaceutical vials, makes this material cheaper and more sustainable, preventing, in turn, the undue filling of landfills. The main drawback is the inhomogeneity of the matrix and the amount of porosity (near to 20%), inducing a very low resistance to crack propagation as compared to the cementitious materials. The modulation of the chemical synthesis (e.g. improving the efficiency of some physical and chemical parameter) and the production of geopolymer matrix composites based on the dispersion fibers, e.g. cellulose and recycled paper ones could be possible solutions to the problem.

Therefore, the aim of this work is to develop and produce an eco-friendly material, with no greenhouse emission, worth of replacing the OPC in building and infrastructural and structural applications, while conferring to the material high strength and fracture resistance by dispersing cellulose and waste paper fibres in the matrix.

According to the overall aim, the following subtasks have been formulated giving a baseline for the research work to be conducted on geopolymers and geopolymeric composites:

- Processing of BSG/FA based GP from waste materials;
- Physical, chemical and mechanical characterization of different formulations of BSG/FA based GPs;
- Optimization of some chemical-physical parameter influencing the reaction;
- Improvement of the reaction efficiency by applying a hydrostatic pressure (HyPS consolidation);
- Processing of cellulose and paper fibers geopolymer composites (GC) by ultra-sonication dispersion of the fibers in geopolymeric matrix;
- Chemical characterization of the interphase between cellulose and geopolymeric matrix;
- Mechanical characterization of GC samples and comparison of the properties with the data from GP characterization.

3. Methodology

3.1 Materials and processing methods

FA was collected from Počerady power plant (North Bohemia, Czech Republic) and thermally treated at 800 °C prior to characterization and alkali activation, in order to burn all the organic impurities out. The loss of ignition was also measured in terms of loss weight percentage of FA. BSG from recycled pharmaceutical vial cullet (Kimble/Kontes, Vineland, NJ, USA) was mixed in different percentage to fly ash in geopolymer processing. The recycled stock of raw borosilicate glass was collected by "Nuova Ompi S.r.l." company (Piombino Dese – Padua). The as-received glass was ball-milled at 350/400 rpm for 15 minutes in an alumina jar with alumina balls (diameter 10 mm) prior mixing with fly ash and alkali activation, using a Pulverisette 6 line planetary ball mill (Fritsch, Germany). The caustic soda (NaOH) was purchased from Sigma Aldrich (Saint Louis, MO, USA). The solid anhydrous compound was provided as pellets with a purity exceeding 97 % (in a form compliant to American Ceramic Society reagent standards).
The cellulose fibers, for geopolymer matrix composite processing, were provided by CIUR A.s. (Brandýs nad Labem, Czech Republic), in a form of dried macrometric fiber. The average length is ca 1.1 mm, the fiber thickness falls in the range of 35 and 45 μm. The density is estimated to be 470 kg/m^3, holding a humidity amount less than 5.5 wt.%. The as-received cellulose fibers were directly mixed with the aluminosilicate suspension, undertaking no other treatments.
The production of the HyPS samples were based on FA and silica gel consolidation. The silica gel powder was obtained by high energy ball milling of silica gel ball for desiccation (350 rpm for 15 minutes). Fused silica microbeads (average diameter of 1.8 μm) were purchased from Cospheric LLC (Goleta, CA, USA) for basic construction of a consolidation model of HyPS process.
GP samples were processed by mechanically dry-mixing FA and BSG powders prior activation in NaOH solution, prepared by dissolving the NaOH pellets in distilled water. The slurry, based on a liquid to solid ratio ranging between 0.3 and 0.4, was then casted in rubber molds and cured in air oven at 85 °C. Six different batches were prepared according to different silica-to-alumina formulation, molarity of the solution and curing time. The description of the batches are reported in table 1.

Table 1: Resume of different adopted terminologies associated to the formulation and curing conditions.

Sample	Fly ash (wt.%)	BSG (wt.%)	Molarity (M)	Curing Time (day)
Mix-1	70	30	13	1
Mix-2	55	45	13	1
Mix-3	40	60	13	1
Mix-4	30	70	13	1
Mix-5	55	45	13	3
Mix-6	55	45	10	1

Samples casting in rubber molds was done in such a way to retain the evaporated water in the curing chamber, as the humidity grade influences the geopolymerization process. For this reason, the airproofing of the samples was accomplished in two manners [9]:

- Method 1: Molds were sealed in latex bags.
- Method 2: Molds were closed in an air-tightened jar with some water.

Irrespective of the methodologies of processing, after curing, the samples were demolded and exposed to air for one week prior to testing in order to complete the geopolymerization. This methodology of preparation was also reported in previous publications [4,10].

The preparation of the GC was based on the Mix-1 formulation, which was properly modified in order to combine the dry mix with cellulose fibers in different percentages (from 1 to 3 wt.%) substituting the FA content (from 69 wt.% to 67 wt.%). The reduction of the FA was not considered sufficient to cause significant change in the properties of the material. The dry mix was then diluted in distilled water and sonicated for one hour to guarantee homogenization of the mix and to unravel the bundles of cellulose fibers. The suspension was dried overnight and the dry mix was activated in a 13 M NaOH solution, forming a slurry whose liquid-to-solid ratio was between 0.8 and 0.9, due to mercerization of the cellulose fibers. The slurry was cast according to method 1 and cured at 85 °C for one day.

3.2 Characterization techniques

Observations of raw materials microstructures (FA and BSG) and the fracture surfaces of both GP and GC samples were carried out through Scanning Electron Microscopy (SEM), model Tescan LYRA 3 XMH FEG/SEM equipped with X-Max80 EDS detector for X-ray microanalysis. Inorganic samples were carbon coated to ensure the sample conductivity.

The chemical composition of the primary materials (FA and BSG) was determined through X-ray fluorescence (XRF) using a RIGAKU (Rigaku Corporation, Tokio, Japan) ZSX100e model operating at 60 kV and 150 mA and equipped with Wavelength-dispersion X-ray spectroscopy (WDS), an X-ray Rh tube working at 3 kW, a scintillation counter for heavy element detection, and a gas-flow proportional counter (Ar–methane 10 %) for the detection of light elements.

The chemistry and the degree of networking of the polymeric structure were evaluated through a simultaneous interpretation of the spectra from FTIR and NMR. FTIR spectra were collected at the Institute of Biomaterials (Erlangen, Germany) by using a Nicolet 6700 FTIR (Walthan, Massachusetts, USA) spectrometer in the range between 4000 and 400 cm^{-1}. The analyses were conducted on pellets composed of 0.2 g of potassium bromide (KBr) and 0.002 g of GP.

^{11}B, ^{27}Al and ^{29}Si NMR spectra were obtained using a Bruker Avance-500 spectrometer (Billerica, Massachusetts, USA), belonging to CEITEC institute (Brno, Czechia). The rotation frequency of 10 kHz was used for 27Al and 29Si, 14 kHz was used for 11B. Recycle delay of 5 s was used for ^{11}B, 2 s for ^{27}Al and 20 s for ^{29}Si. ^{29}Si NMR spectra were deconvoluted in the sum of the single chemical shifts, using the DMfit software [11]. The admitted error was calculated to be about ±1 ppm.

XRD spectroscopy was instrumental to qualitatively and quantitatively inspect the crystalline part of the FA and GP samples. XRD patterns were collected using X′Pert Pro (PanAnalytical, Netherlands) powder diffractometer with Bragg-Brentano (theta-theta) geometry, operating with Co Kα _1.2 radiation. It is equipped with a 1-D linear detector and β -filter.

The evaluation of the grain size of the FA and BSG powders was carried out by means of laser diffraction particle sizing technique, using a Malvern Hydro2000MU (United Kingdom), and located in SASIL S.P.A. facilities (Italy).

The relative density (ρ_{rel}) of each sample was calculated by measuring the actual density of the samples through the geometrical method and assessing the theoretical density of the GP samples. The theoretical density was weighted according to the GPs formulations (Table 3). The theoretical densities of FA (d_{FA}) was calculated starting from the density of the single source (i.e. FA and BSG), which were measured by means of an automatic pycnometer PYCNOMATIC ATC (VŠB - Technicka Univerzita Ostrava). The proportion of open and closed porosity was deduced by means of the Archimede's method, using high purity distilled water as buoyant. The weighting of the specimens was carried out using a Denver analytical balance (±0.0001 g resolution) [12].

The determination of the compressive strength of the GP samples was performed through compression test carried out on 5 mm x 5 mm x 10 mm prismatic specimens, appropriately cut from demoulded Mix-1 and Mix-2 type GP samples (see Table 1). The specimens were tested not earlier than one week after demoulding, in order to complete the geopolymerization. The setup on compression test was mounted on a universal test system INSTRON 8862 testing machine (Norwood, Massachusetts, USA), carrying a system load cell capacity up to ± 100 kN with optional load cells with smaller capacity down to 200 N. The speed rate of the cross-head was set to 0.5 mm/min.

A set of 10 prismatic specimens of the size 4 mm x 3 mm x 16 mm were tested in a three-point bend configuration (3PB) so as to assess the flexural strength, according to the standards ASTM D790-17 [13]. The data scatter was based on the interquartile range (IQR), with a factor of 1.5. The configuration of the 3PB test comprehends three rollers (5 mm in diameter), mounted two below and one above the sample. The tests were carried out on a screw-driven testing Zwick Z50 machine (Ulm, Germany) with load cell capacity up to ± 50 kN with optional load cells with smaller capacity down to 200 N. The speed rate of the cross-head was set to 10 μm/min. Deflection was measured by inductive transducer incorporated directly into loading axis. The same configuration was applied to 10 specimens with equal size of the 3PB specimens in chevron notch technique, according to the methodology reported in the literature [14]. 10 μm/min was set as the cross-head speed for all the tested specimens

The instrumented micro-indentation experiments were performed on produced Mix-1 and Mix-2 GP samples after one month of curing in the air (room temperature) using a screw-driven ZWICK Z2.5 testing machine (Ulm, Germany) equipped with micro-hardness head ZHU0.2 with optics.

4. Main results

4.1 Description of the raw materials

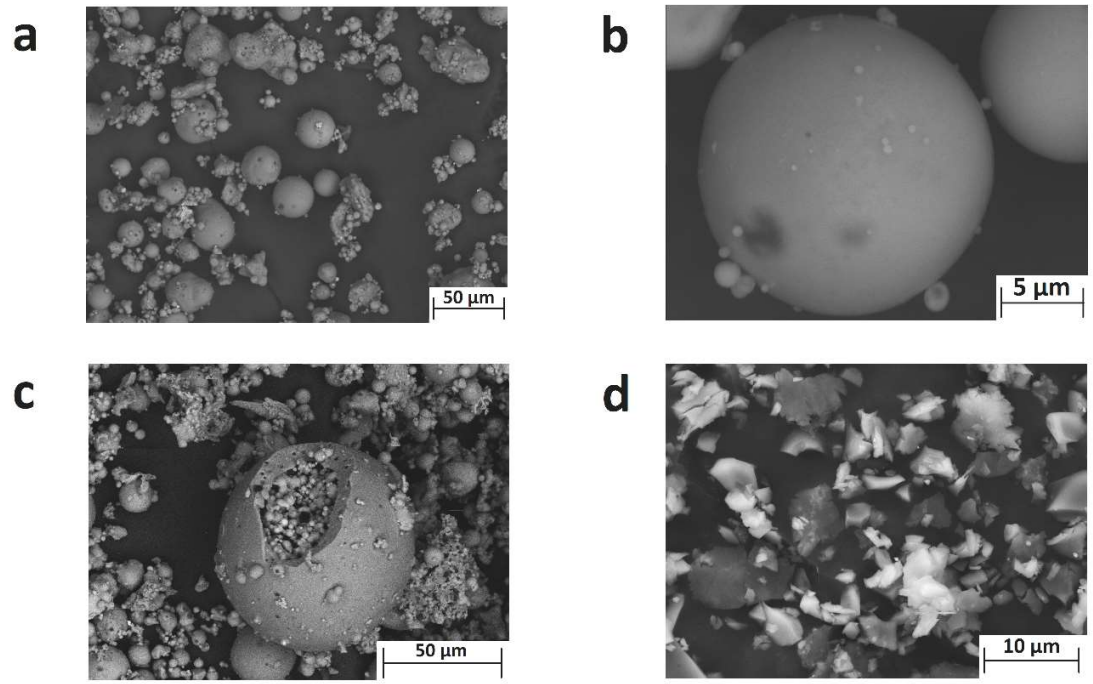

Figure 1: Scanning electron micrographs of the a) fly ash, b) fly ash particle, c) hollow fly ash particle and the d) borosilicate glass.

The FA is known to be largely heterogeneous, being a by-product of ignited fossil fuel. The diversity in microstructure and the wide presence of impurities are also visible from the SEM micrographs reported in Figure 1 a-c, where the microstructure is characterized by shapeless particles and almost perfect spheres (Figure 1a), associated with aluminosilicate and silicate particles. Figure 1b depicts a close up of one of these particles, whose surface looks perfectly smooth at the SEM, meaning that most of them have a glassy nature. Other important peculiarities are that, very often, they are also surrounded by smaller FA particles and that these spheres are mainly hollowed, and densely composed by a large deal of smaller FA sphere-like particles from inside (Figure 1c). This morphology may help the reactivity of the FA during alkali activation, as once the outer shell is chemically attacked, the activator comes into contact with smaller particles with a higher specific surface, improving the dissolution of the FA. The microscopic appearance of the BSG powder (Figure 1d) is of random shape particles, typical of a brittle material processed through high energy ball milling. The high energy ball milling in alumina jar/balls is an efficient method to achieve micrometric grain size and suitable particles distribution.

Table 2: Chemical composition of raw fly ash and borosilicate glass.

	SiO_2	Al_2O_3	B_2O_3	Fe_2O_3	CaO	K_2O	Na_2O	L.O.I [1]	Residues
Fly ash (wt.%)	46.3	26	-	13.9	3.5	3.9	0.2	0.7	5.5
BSG (wt.%)	72	7	12	-	1	2	6	-	-

[1]Loss of ignition (L.O.I.) – calculated through weight loss after fly ash firing.

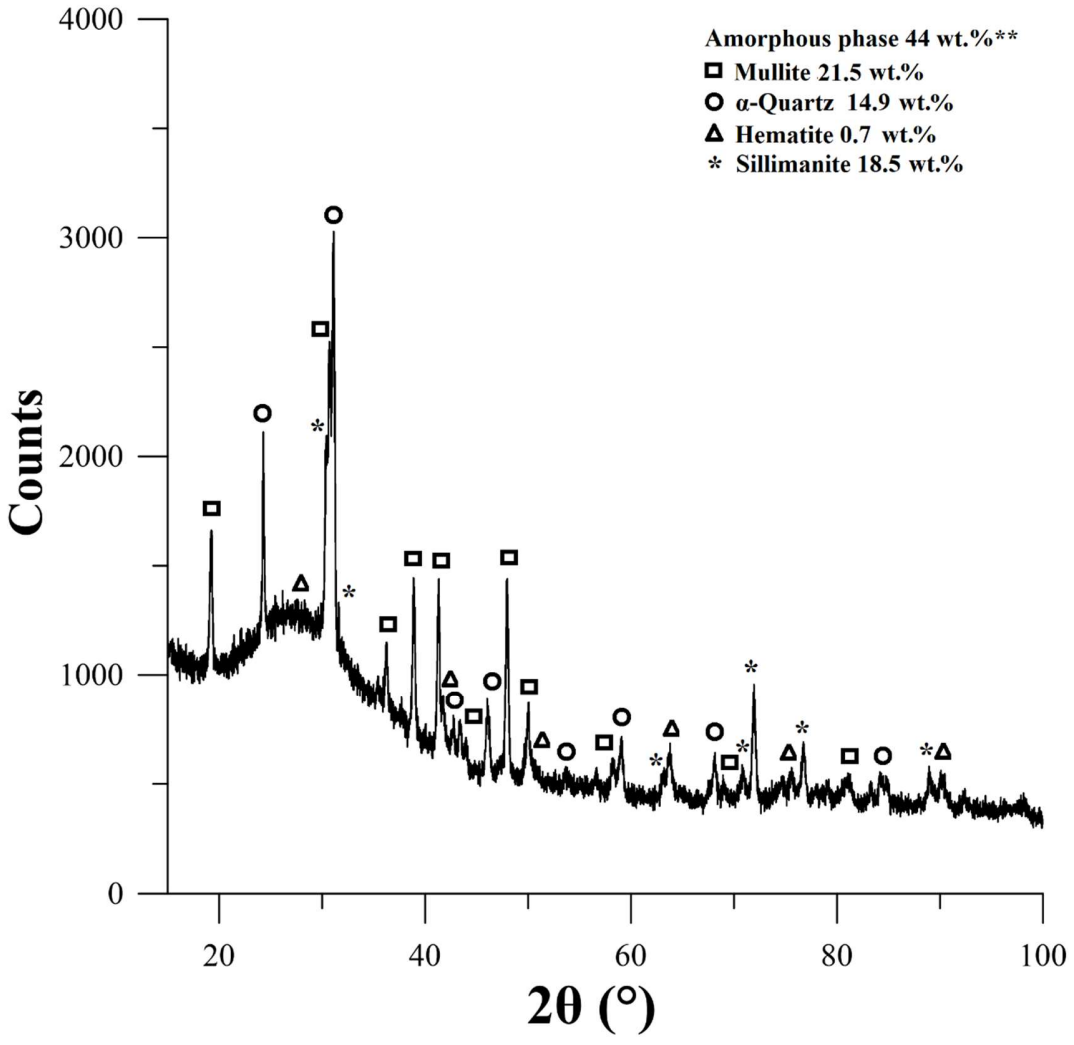

Figure 2: X-ray diffraction spectroscopic spectra of the fly ash. **Amorphous phase calculated through internal standard method [15]**.**

The chemical composition was determined through fluorescence X-ray (XRF) spectroscopy and the results are reported in Table 2. The content of calcium oxide (lime) was lower than 15 wt.%, render this FA classifiable under the notation class F, according to the international standards related to coal derivatives [16,17]. The composition of BSG reported in Table 2 evidenced a reactive silica content (72 wt.%), almost double than the FA, ensuring an easiness in chemistry adjustment with less consumption of material. Moreover, the presence of a low amount of alumina (7 wt.%) does not influence negatively this aspect. More interestingly, the high presence of borates in the chemical composition (12 wt.%), capable of participating in the reaction seemingly to alumina compound.

The crystalline phases of the tested material are readily determined by peaks fitting of XRD spectrum of FA, reported in Figure 2, while the glassy phase is determined through the internal standard method [18]. The internal standard method revealed a glassy content of 44 wt.%, causing a large hump comprehended between 20° and 40° (°2theta) in the XRD spectrum. The crystalline part of the FA is mainly composed by mullite ($Al_6Si_2O_{13}$) for the 21.5 wt.% of the crystalline portion of the FA, the sillimanite ($Al_2(SiO_4)O$) covering the 18.5 wt.% and the α-quartz (SiO_2) phase accounting for the 14.9 wt.% of the total crystalline phase (see Figure 2). The 14 wt.% of the iron oxide, reported in the chemical composition is ascribed to hematite (Fe_2O_3) evidenced in the XRD spectrum, whose weight contents was 0.7 wt.%. This value of the iron oxide content detected through XRD is controversial, giving the 14 wt.% of Fe_2O_3 detected through XRF spectroscopy (Table 4).

The grain size of the powders was measured using the Brunauer-Emmet-Teller (BET) method (Table 3). When lower energy ball milling was used (350 rpm), the available specific surface area was calculated to be 0.23 m^2/g, but this value considerably increases up to 0.71 m^2/g if the powder was milled at 400 rpm. The BET analysis of FA showed a value of 2.65 m^2/g, which is more than three times higher than the high energy ball-milled BSG value. In preparation of GP samples only 400 rpm ball milled BSG was employed.

Table 3: Density, specific surface and grain size (50 % of probability) of the fly ash and borosilicate glass milled according to two different rotating speeds (350 and 400 rpm).

Powder	**Density (g/cm^3)**	**BET* Specific Surface area (m^2/g)**	**Grain size d_{50} (μm)**
Fly ash	2.35	2.65	22.24
BSG (350 rpm)	2.23	0.23	/
BSG (400 rpm)	2.23	0.71	5.09

* Brunauer-Emmet-Teller method

4.2 Preparation and characterization of geopolymers

Microstructure of the geopolymer samples

The comparative analysis of the microstructure of the GP samples (from Mix-1 to Mix-6, see Table 1) is reported in Figure 3. Mix-1 (Figure 3a) presents a regular amount of pores and cracks, but when the BSG content in the formulation is increased, as in Mix-2 in Figure 3b, the presence of cracks visibly increases, while the porosity seems to remain the same. In Mix-3 (Figure 3c), the BSG content was increased up to 60 wt.%, thus inducing an apparent increase of both the porosity and cracks, but the microstructure gets better if a Mix-4 formulation is adopted, as reported in Figure 3d. The increase of the curing time of the Mix-2 formulation, giving rise to Mix-5 sample (Figure 3e) is accompanied by a formation of larger closed pores, a characteristic equally observed also in Mix-6 (Figure 3f).

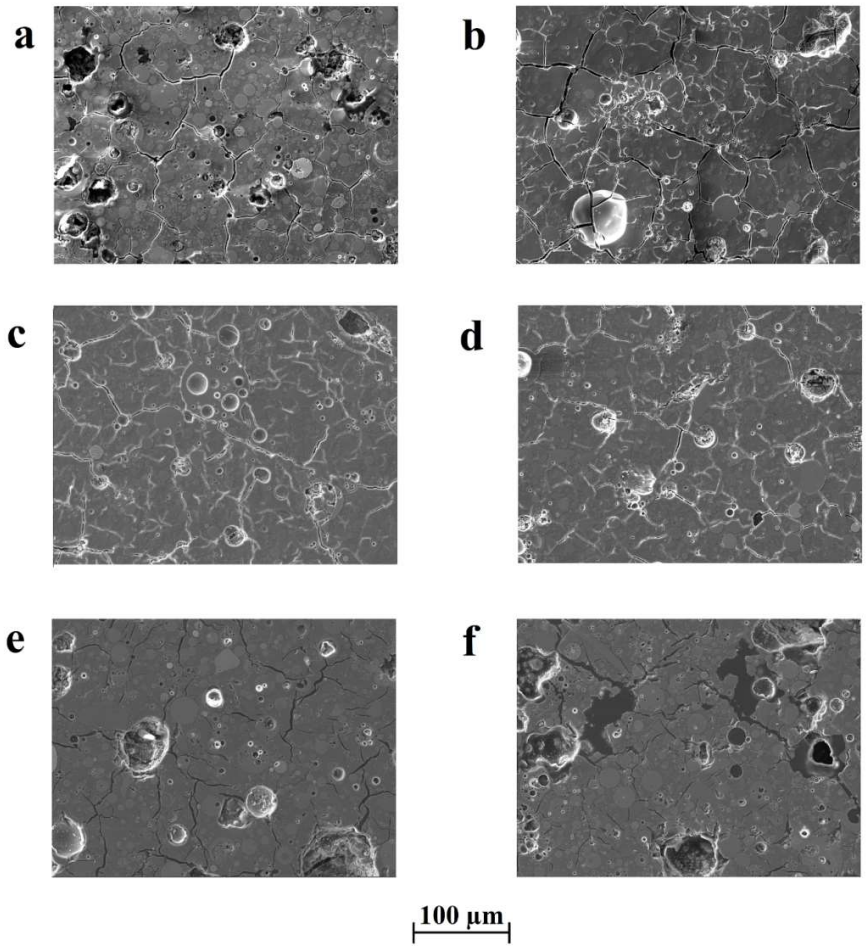

Figure 3: Secondary electron pictures of the polished surfaces of a) Mix-1, b) Mix-2, c) Mix-3, d) Mix-4, e) Mix-5 and f) Mix-6. All the images were reported with the same magnification (the marker applies for each picture).

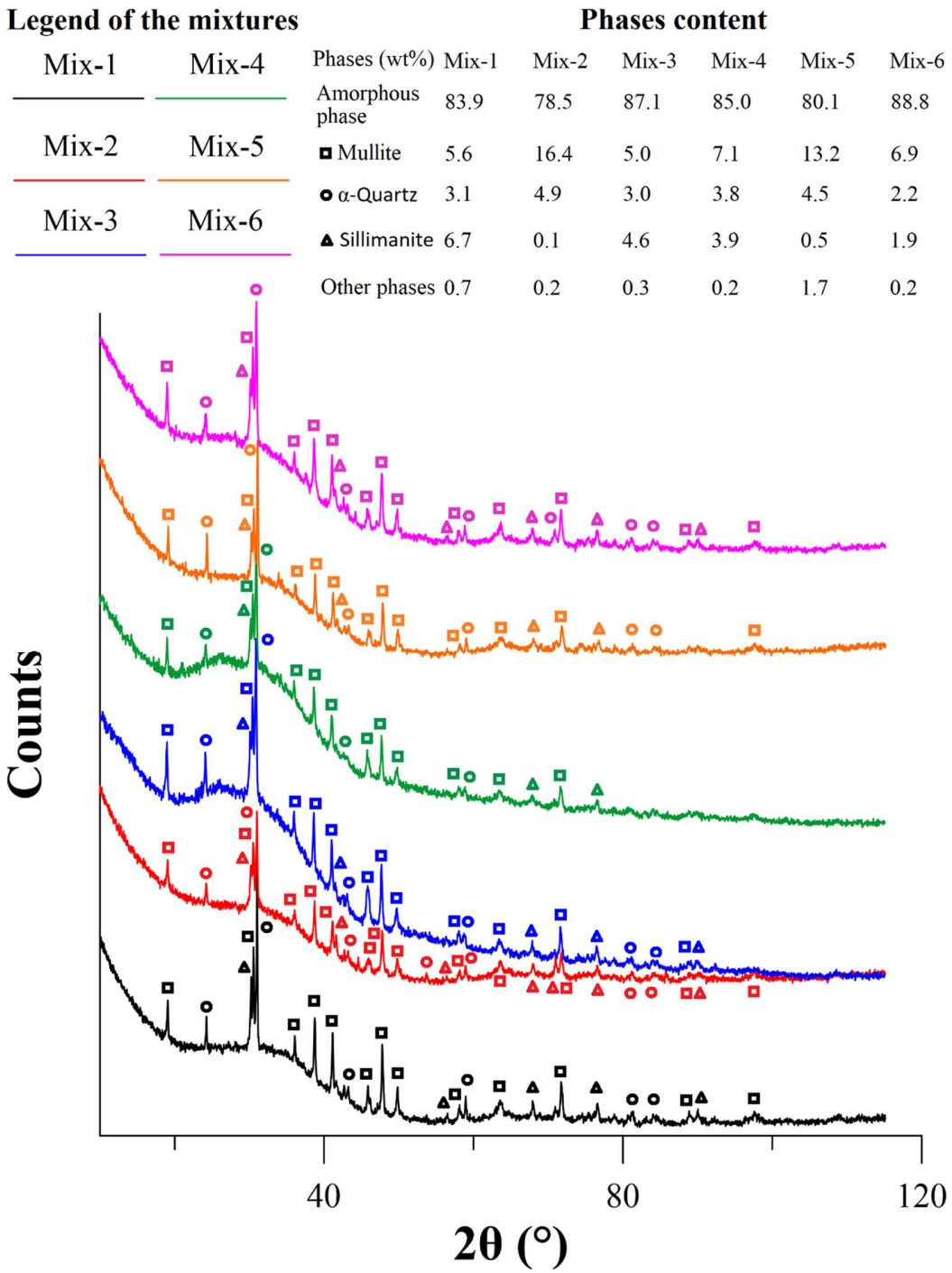

Figure 4: A comparison of the X-Ray diffraction spectra of the GP samples (from Mix-1 to Mix-6).

Spectroscopic analysis of geopolymers

The amorphous and crystalline phases are provided by the XRD spectra of the GP samples in Figure 4. The amorphous phase amount decrease from Mix-1 (83.9 wt.%) to Mix-2 (78.5 wt.%), having a higher amount of BSG. The same could be uttered for the amorphous amount of Mix-3 and Mix-4 (87.1 and 85.0 wt% respectively). From this observation, it is deduced that the crystalline phases of FA are active contributors in geopolymerization. The mullite and the sillimanite phases display no smooth trend of their content from Mix-1 to Mix-4 (Figure 37), especially showing depletion of sillimanite when the mullite is higher in percentage, like happening in Mix-2 (mullite 16.4 wt.% and sillimanite 0.1 wt.%). The trend of α-quartz content remains approximately constant through the spectra, suggesting very limited contribution of this phase to dissolution.

Observing the Mix-5 and Mix-6, it was noticed that a higher amorphous content results in 10 M NaOH solvent, i.e. 88 wt.%, coinciding also with the larger amount of amorphous phase among all the mixtures. For a longer time of curing, a higher formation of crystallinity was detected (80.1 wt.%. Indeed, the Mix-5 holds a considerable percentage of mullite (13.2 wt.%), almost as high as the Mix-2 (6.4 wt.%, the highest), most likely part formed during geopolymerization. In Mix-5, the tendency to have almost depleted sillimanite (0.5 wt.%) higher content of mullite with respect to the average repeats. Low content of sillimanite was detected also for Mix-6, though the mullite content is moderate, suggesting that the extensive formation of the amorphous phase is followed by a limited formation of crystals. The content of crystalline silica is approximately constant.

In Figure 5 are depicted both the FA and the GP sample spectra. Starting from the FA spectra, the most meaningful absorption picks are below the 1000 cm^{-1} wavelength, but most parts of the bond vibrations fall in the mid-IR region. According to Sitarz et al., the 6-membered rings have a characteristic absorption band within 550 and 600 cm^{-1}, the 4-membered ring at about 640 cm^{-1} and the 3-membered ring within 720-700 cm^{-1} [19,20]. In the FA spectrum, an intense absorption band is evident at ca. 555 cm^{-1}, meaning that the FA holds a sizeable amount of the 6-membered ring elements. The band at 466 cm^{-1} is, instead, related to in-plane bending vibration of Al-O and Si-O oligomeric species [21,22].

The GP spectrum present more absorption bands than the FA spectrum at higher wavelengths, whereas it remains almost unchanged in the mid-IR region. The characteristic band is, instead, shifted slightly towards lower wavelengths (1010 cm^{-1}), suggesting that the geopolymeric matrix might have a less intricate network, with a higher level of hydration (more Si-OH terminal bonds) [23]. This observation was confirmed by the broad band between 2066 and 3400 cm^{-1} associated with stretching vibration of –OH group (silanol). The band at 1644 cm^{-1} is attributed to constitutional water, related to bending vibration of the H-O-H bonds [20,23–25]. The effect of the efflorescence reveals at the GP spectrum through the 1460 cm^{-1} absorption band, attributed to the bending vibration of O-C-O bonds (carbonation) [24,26]. Finally, a small shoulder was detected at 820 cm^{-1}, associated with the vibration of the B-OH tetrahedral boron species.

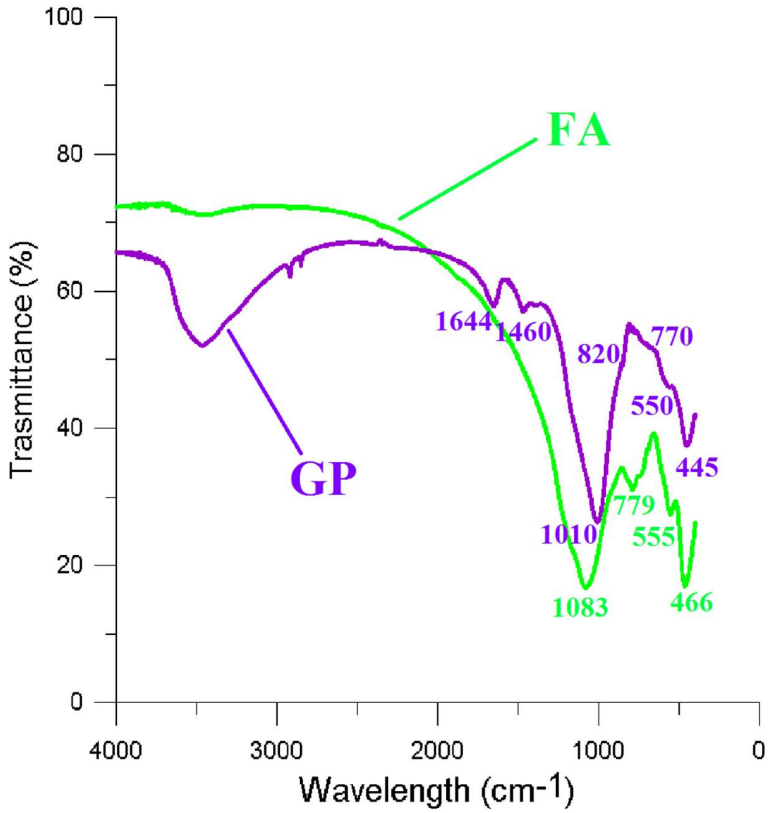

Figure 5: Fourier transform infra-red spectroscopy of the fly ash (FA-green solid line) and the Mix-1 geopolymer (GP-purple solid line).

The comparative study of the ^{29}Si MAS NMR spectra of FA and GP is reported in Figure 6. Starting from the FA spectrum, one can notice that it holds several signals at high ppm and an intense one at -110 ppm. The resonance signals from -84 to -104 ppm are related to the different vitreous and crystalline structure of the Si in Q^2 and Q^3 configuration [4,11,25,27]. The -100 ppm peak is a $Q^4(0Al)$ amorphous ambient, whereas the shoulders produced by the -114 and -118 ppm are the crystalline configuration of the same ambient [4,11,27]. the resonances associated with low ppm signal (from -100 ppm to -115 ppm) are mainly $Q^4(0\text{-}1Al)$ species, whereas at high ppm, the signals may be attributed to Al-rich silicate species ($Q^4(2\text{-}4Al)$) [11,27].

The ^{11}B MAS NMR spectroscopy was performed on raw BSG and GP sample, whose plots are shown in Figure 7. The intense hump characterizing both spectra is a background noise due to the interference of the borosilicate-based rotor mounted in the NMR machine – being equally intense for both the analyses, it is easily ignored. The BSG spectra (blue solid line) evidences two main peaks – one at +10 ppm attributed to trigonal coordinated boron, and one more intense at 0 ppm related to the resonance of the tetrahedral coordinated boron [28–31]. The GP sample spectroscopy (red solid line Figure 7) leaded to a spectra almost nil in +10 ppm resonance signal

in favour of a more intense 0 ppm signal, demonstrating for the first time that the boron is an active element in geopolymerization process, and the borates are building blocks of the inorganic polymeric network resulting from the polycondensation reaction [4].

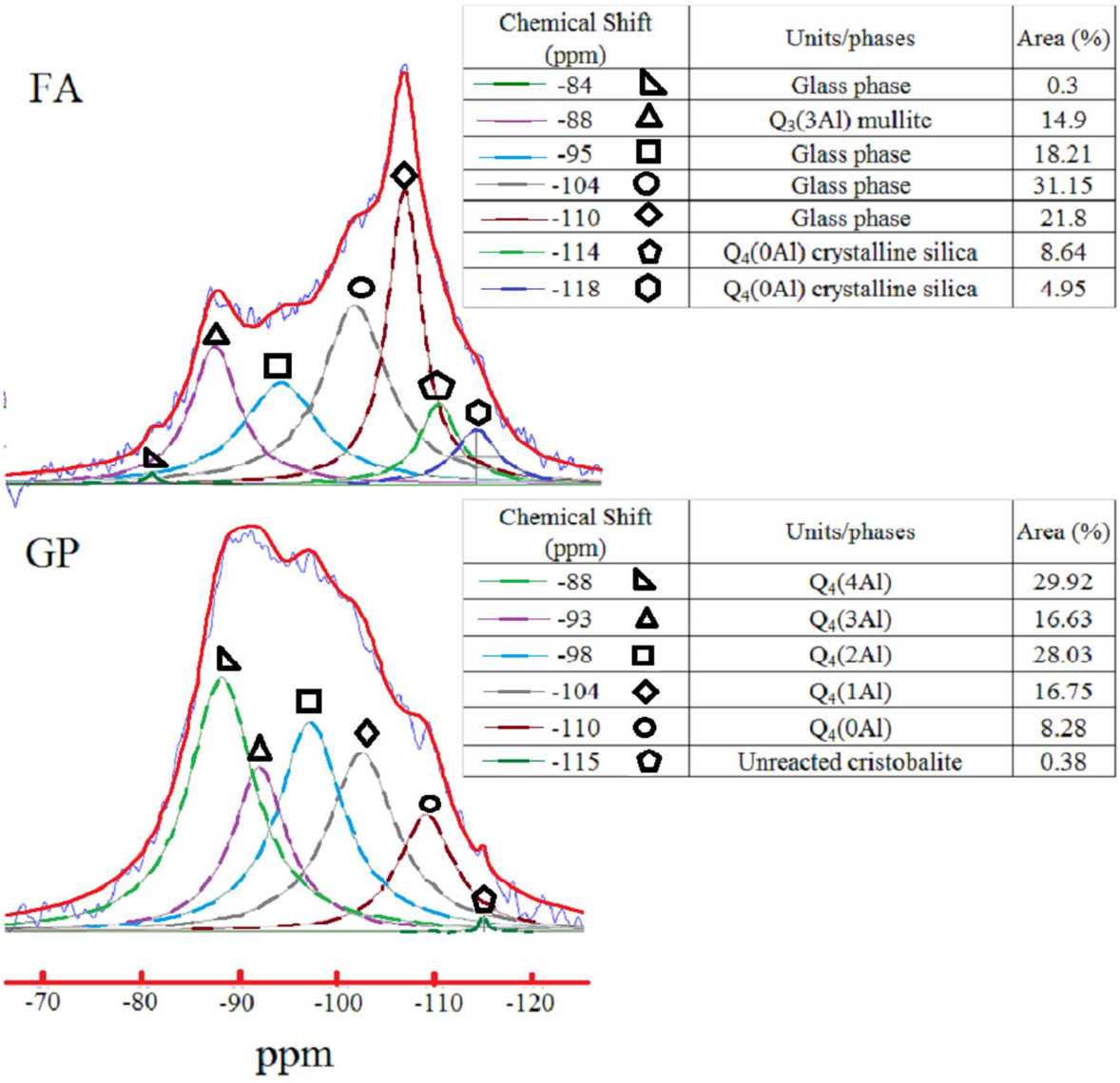

Chemical Shift (ppm)	Units/phases	Area (%)
-84	Glass phase	0.3
-88	$Q_3(3Al)$ mullite	14.9
-95	Glass phase	18.21
-104	Glass phase	31.15
-110	Glass phase	21.8
-114	$Q_4(0Al)$ crystalline silica	8.64
-118	$Q_4(0Al)$ crystalline silica	4.95

Chemical Shift (ppm)	Units/phases	Area (%)
-88	$Q_4(4Al)$	29.92
-93	$Q_4(3Al)$	16.63
-98	$Q_4(2Al)$	28.03
-104	$Q_4(1Al)$	16.75
-110	$Q_4(0Al)$	8.28
-115	Unreacted cristobalite	0.38

Figure 6: ^{29}Si magic angle spinning nuclear magnetic resonance spectra of fly ash and geopolymer sample Mix-1.

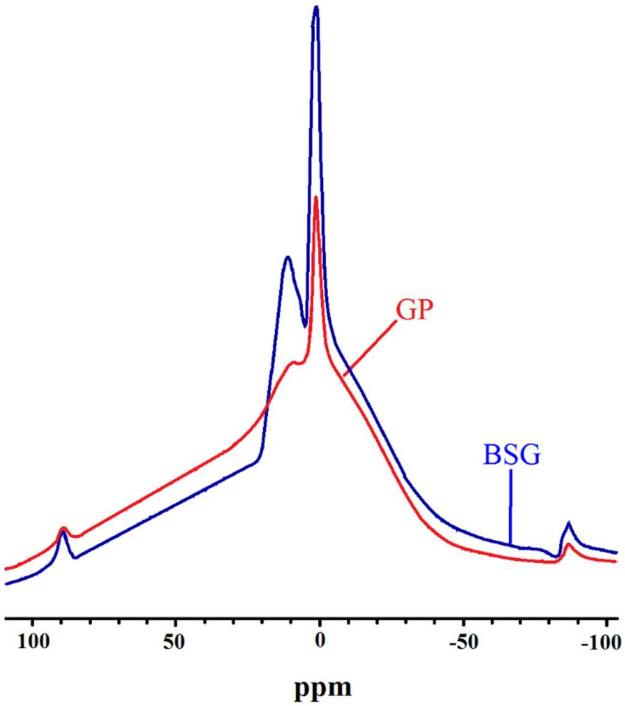

Figure 7: ^{11}B magic angle spinning nuclear magnetic resonance of the borosilicate glass and the Mix-1 geopolymer sample.

Density evaluation of the geopolymers

The relative density was measured through the volumetric evaluation of the samples and theoretical density calculation (Table 4). It was found that the relative density is the highest one (87.1%) when the mix contains a lower amount of BSG in formulation (Mix-1) (lower silica to alumina ratio), and goes down as the BSG content is raised (Mix-2 and Mix-3), and again it raises (86.4 % in Table 4) when the BSG content is as high as 70 wt.%. Therefore, the highest amount of porosity coincides with the Mix-3 batch (relative density of 81.5 %), containing 60 wt.% of BSG.

Mechanical properties of geopolymers

Compression test (10 specimens) and microindentation hardeness test (10 indentations) were conducted on samples Mix-1 and Mix-2, and reported in Table 5. The results of the compression test evidence higher compressive strength (45 MPa) if higher content of BSG is used in formulation (Mix-2). The Mix-1 sample revealed a compression strength about 10% lower than Mix-2 (39 MPa). The results of the micro-indentation test evidenced an average value of 78 for Mix-2 sample, slightly higher than Mix-1, which showed an indentation hardness of 73 HV.

Table 4: Formulations (fly ash and borosilicate glass mixture) adopted in geopolymer samples manufacturing and relative parameters (silica-to-alumina "SiO_2/Al_2O_3" ratio and relative density "ρ_{rel}").

Sample	FA–BSG (wt.%)	SiO_2/Al_2O_3	ρ_{rel} (%)
Mix-1	70–30	2.7	87.1
Mix-2	55–45	3.3	84.4
Mix-3	40–60	4.2	81.5
Mix-4	30–70	5.0	86.4
Mix-5	55–45	3.3	82.9
Mix-6	55–45	3.3	77.4

Table 5: Compression strength and indentation hardness of geopolymer samples.

Sample	Compressive strength (MPa)	Hardness (HV)
Mix-1	39	73
Mix-2	45	78

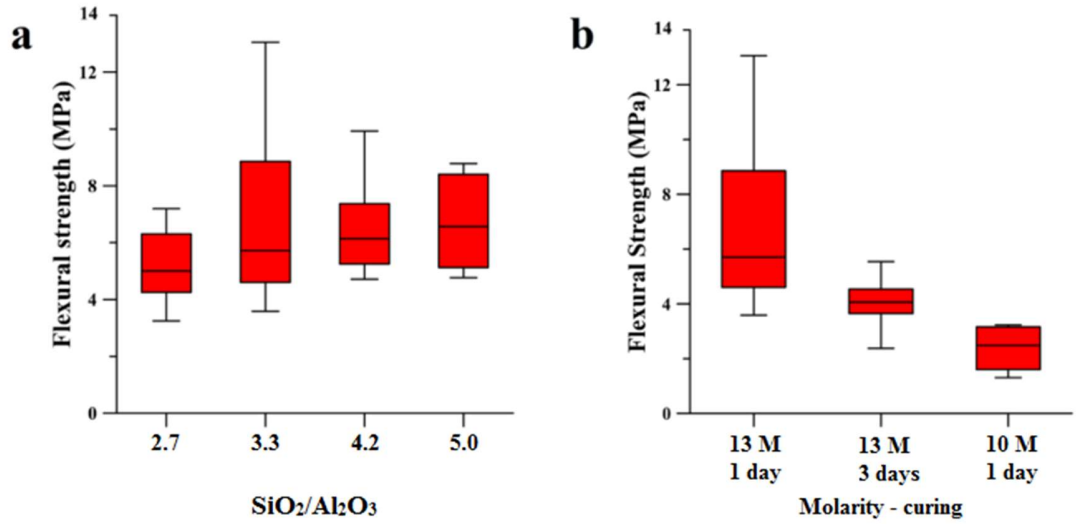

Figure 8: Flexural strength of geopolymer samples in terms of (a) silica-to-alumina ratio of the mixtures from Mix-1 to Mix-4 (2.7, 3.3, 4.2, 5.0 respectively) and (b) molarity of the activator and curing time used for Mix-2 (13 M for 1 day), Mix-5 (13 M for 3 days) and Mix-6 (10 M for 1 day).

The influence of the SiO_2/Al_2O_3 ratio on the flexural strength is evidenced in Figure 8a, which reports the bending test results of the mixtures subjected to a different formulation (from Mix-1 to Mix-4). It was observed that the highest flexural strength (12 MPa) was obtained for Mix-2

formulation (FA-BSG 55-45 wt.%). The Mix-5 and Mix-6 in Figure 8b take in consideration the effect of the molarity of the alkali solution (10 M) and the curing time (3 days) respectively, and the results were put in comparison with the Mix-2. It was found that both the reduction of molarity of the solution and the longer curing time were detrimental for the flexural strength of the GP samples, displaying a bending resistance up to 2 times for Mix-5 and 3 times for Mix-6 lower than the Mix-2.

4.3 Cellulose based geopolymer composites

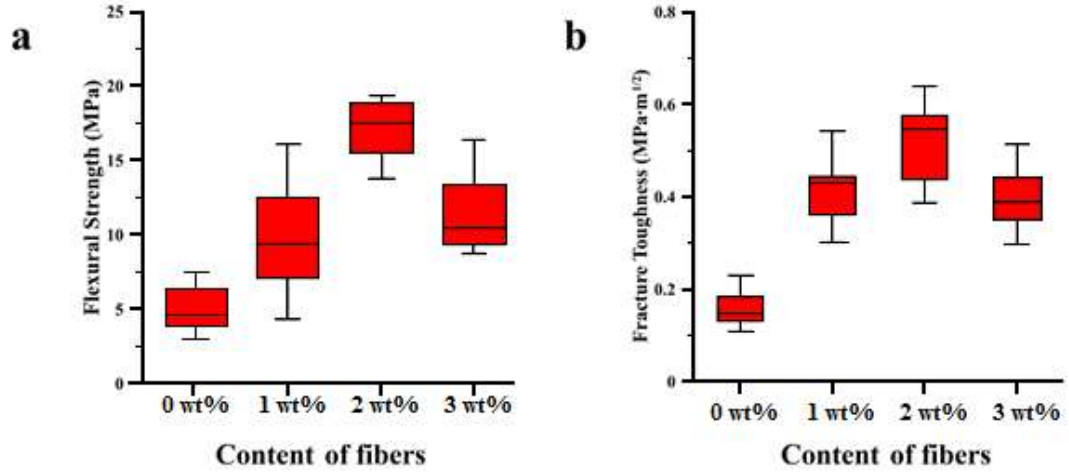

Figure 9: a) Flexural strength and b) fracture toughness of the geopolymer matrix composite.

One of the ways to increase bending strength and fracture toughness of a material is to produce composites. GC were produced by dispersing cellulose fibres in the GP matrix and samples were tested in 3PB and CVN tests. The results of the 3PB test are reported in Figure 9a, showing that the highest flexural strength (20 MPa) is achieved when 2 wt.% of cellulose fibres are randomly dispersed in the geopolymeric matrix. Comparing these results with those in Figure 8, it was observed that the GP composite attains a resistance to bending stress almost double than the Mix-2 sample, and even 5 times higher than Mix-1 sample. The samples with 1 wt.% and 3 wt.% of cellulose displayed a similar flexural strength, but anyway lower than that with 2 wt.%. The assessment of the fracture toughness of the samples from the chevron notch test provided similar results as the flexural strength (Figure 8b) – the higher fracture toughness is related to the 2 wt.% of cellulose sample, having a critical stress intensity factor up to almost 0.7 $MPa \cdot m^{1/2}$. This value was found to be more than 3-fold higher than the fracture toughness measured on Mix-1 sample (see Figure 46b). Micrographs carried out on polished and fracture surface of the GC samples also evidenced a sort of interaction between the geopolymeric matrix and the polymeric structure of the cellulose, presumably affecting the mechanisms of fibres pull-out and crack bridging.

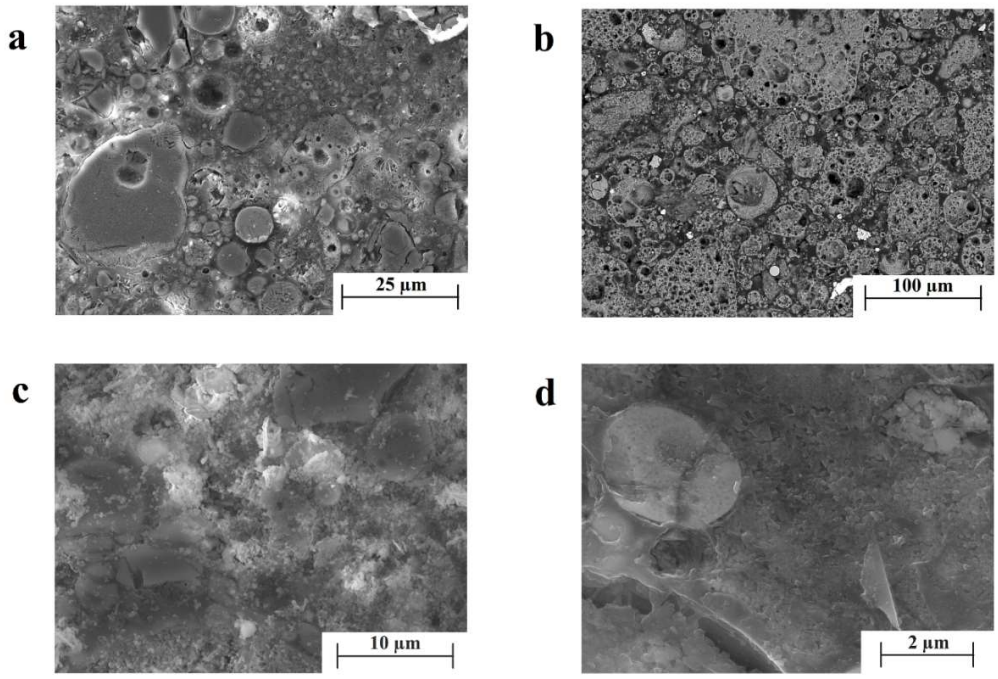

Figure 10: Scanning electron microscopy of fly ash densified in according to the hydro-pressure sintering process under 500 MPa for 5 minutes in a) water, b) 3M NaOH solution, c) 5M NaOH solution and d) a detail of the crystals of the sample processed in water.

4.4 Hydro-pressure sintering

The microstructure of the FA based HyPS samples processed in water and NaOH solution (3M and 5M) under 500 MPa of hydrostatic pressure and kept in these conditions for 5 minutes was observed at the scanning electron microscope and reported in Figure 10. The morphology of the polished surface of all the samples, at a first sight, seemed nicely densified, similarly to a normal geopolymerization, but some differences are rising from the microstructural observation. Among all, the product of geopolymerization holds a more crystalline morphology, with an extensive presence of needle-like and sponge-like crystals (see Figure 10c and d). This was particularly more evident in the NaOH 5M HyPS and water HyPS sample – especially the latter was surprising, as the formation of crystals in GPs was often connected to the presence of Na^+ cations, forming zeolitic crystalline precursors [32].
This observation is motivated by the effect of the Ostwald ripening mechanisms – the migration and reorganization of the species (recrystallization) onto bigger particles could involve the formation of more crystals. Nevertheless, the formation of crystals was an unexpected result, as the release of pressure and the fast drying of the sample should retain the metastable microstructure. Being the liquid phase a highly concentrated solution of aluminosilicate species, it was, instead, expected that the microstructure would have showed an amorphous aspect. From

Figure 10, it was observed that this is not the case for FA-based samples, irrespective of the type of solvent.

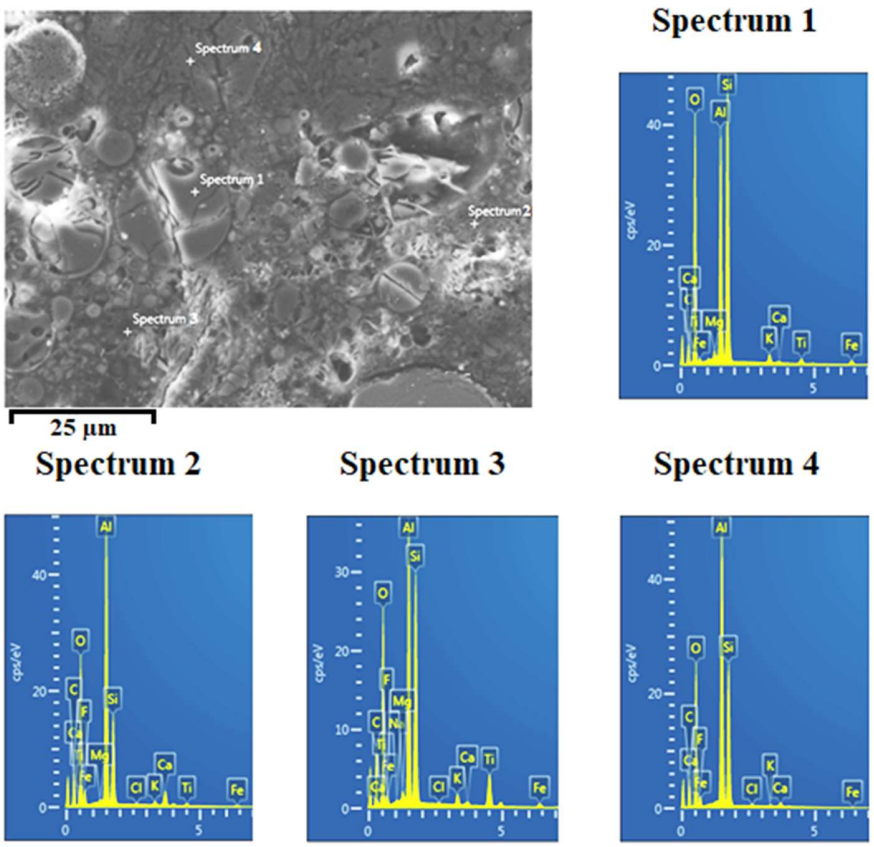

Figure 11: Energy dispersive spectroscopy analysis of the fly ash HyPS sample processed in water.

The spectroscopic analysis of the microstructure was further integrated with the chemical information provided by the energy dispersive microscopy (EDS) performed on the FA HyPS sample processed in water (Figure 11). The spectrum 1, associated with an aluminosilicate undissolved particle, was put in comparison with the chemical composition of the product of geopolymerization in several points (spectrum 2, 3 and 4 in Figure 11), appropriately selected to investigate both the amorphous and the crystalline sites. The glassy phase of the geopolymeric product (spectrum 3 and 4) was found to have a higher content of aluminium if compared to the GP matrix (Figure 38), but this was expectable as the GP formulation comprehended both FA and BSG. Interestingly, the chemical composition of the crystalline site (spectrum 2) is visibly richer in aluminium, even double than the silica content, conceivably attributable to the formation of sillimanite phases.

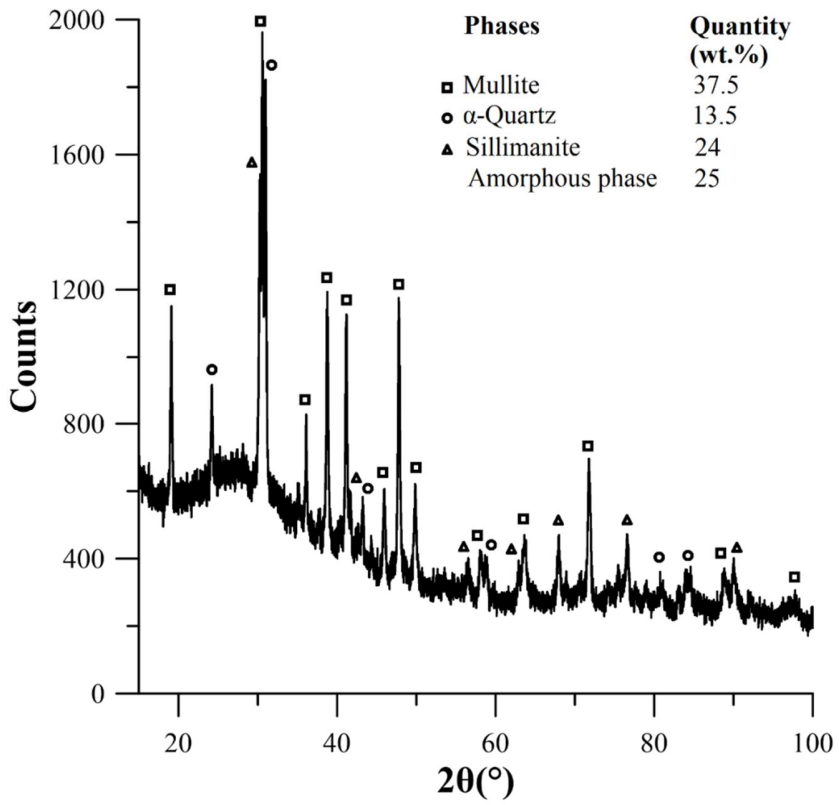

Figure 12: X-ray diffraction spectrum of the fly ash based HyPS sample.

To demonstrate this observation, the same sample was examined to the X-ray diffraction spectroscopy, in order to quantitatively and qualitatively define the crystalline phases produced after the process. The XRD spectrum of the FA based HyPS sample consolidated in water is reported in Figure 12. The fitting of the spectrum peaks evidenced a large presence of aluminosilicate crystalline phases, such as mullite ($Al_6Si_2O_{13}$) and sillimanite (Al_2SiO_5) (37.5 and 24 wt.% respectively), consistent with the EDS results.

Compared to the XRD spectrum of the FA sample (Figure 2), the level of the quartz phase is almost unvaried. The hematite was negligible, similarly to FA (the iron oxide is not expected to react irrespective of the process). The major difference between the two spectra resides on the sillimanite and mullite contents, which are 18.5 and 21.5 wt.% in the FA sample, as reported in Figure 2. This could suggest part of the amorphous phase contained in FA dissolves and recrystallizes in the form of mullite and sillimanite (a mechanism well explained by the Ostwald ripening). Indeed, one might observe that the characteristic halo associated with the amorphous phase in the FA spectrum (Figure 2) hold a halo falling in the range of 25° and 40°. The FA-based HyPS sample spectrum characteristic hump not only is slightly shifted to the left (20° - 35° 2θ) but it is also associated with a less amount of glassy phase in microstructure (55 wt.% through internal standard method).

5. Conclusion

New geopolymer was designed by incorporation of fly ash and borosilicate recycled glass, evidencing an improvement in compressive strength of about 25 % as compared to geopolymers based on fly ash and recycled glass (e.g. urban glass) reported in the literature. The silica to alumina (SiO_2/Al_2O_3) ratio was tuned so as to find the best formulation. The bending test evidenced the highest flexural strength for a ratio of 3.3 (12 MPa - Mix-2). Alkalinity of the solvent and curing conditions were also inspected, revealing best performance in terms of flexural strength for a 13 M caustic soda solution, cured at 85 °C for 1 day in sealed condition for a given formulation. The chemistry of the material was investigated through FTIR and NMR spectroscopy, showing a shift of the characteristic FTIR peak (~ 1000 cm^{-1}) towards higher wavelength and of the ^{29}Si NMR hump toward lower ppm as the silica to alumina ratio is increased. ^{11}B NMR spectra demonstrated that borates contained in the borosilicate glass play an active role in the geopolymerization similar to aluminates.

Geopolymer matrix composites with dispersed cellulose fibres on the basis of the fly ash and borosilicate glass formulation and dispersing cellulose fibres by ultra-sonication were successfully produced. Improvements in flexural strength and fracture toughness of about 162 % and 51 % respectively as compared to plain geopolymer formulation were achieved, rendering this material more suitable for structural applications. Cellulose fibres were superficially modified by the geopolymeric matrix, establishing an intermediate layer between the two materials. The formation of this affected zone suggests a sort of interaction between the organic polymer and the geopolymeric compound.

A new room-temperature pressure-driven method of power densification, named hydro-pressure sintering, was developed using the simoultaneous effect of the dissolution from an aqueous solvent and the effect of the pressure (this method has been submitted in a patent application Nr. D18079023). The dynamics of densification are characterized by the preferential dissolution, migration and re-precipitation of dissolved aluminosilicate species driven by the mechanisms of the Ostwald ripening. Fly ash was successfully densified up to 80 % of relative density, under 500 MPa for 5 minutes in water and NaOH (3M and 5M) solutions, thus allowing the utilization of less aggressive solvents. The observation of the microstructure through scanning electron microscope evidenced formation of crystals, likely induced by the pressure. The XRD spectroscopy corroborated this observation, revealing the presence of aluminosilicate crystalline phases (mullite and sillimanite), and lower content of the glassy phases forming during conventional geopolymerization.

6. References

[1] F. Pacheco-Torgal, J. Castro-Gomes, S. Jalali, Alkali-activated binders: A review. Part 1. Historical background, terminology, reaction mechanisms and hydration products, Constr. Build. Mater. 22 (2008) 1305–1314. doi:10.1016/j.conbuildmat.2007.10.015.

[2] B. Singh, G. Ishwarya, M. Gupta, S.K. Bhattacharyya, Geopolymer concrete: A review of some recent developments, Constr. Build. Mater. 85 (2015) 78–90. doi:10.1016/j.conbuildmat.2015.03.036.

[3] ECOBA, Torwards a thematic strategy on the prevention and recycling of waste, (2001) 5.

[4] G. Taveri, J. Tousek, E. Bernardo, N. Toniolo, A.R.R. Boccaccini, I. Dlouhy, Proving the role of boron in the structure of fly-ash / borosilicate glass based geopolymers, Mater. Lett. 200 (2017) 105–108. doi:10.1016/j.matlet.2017.04.107.

[5] D. Khale, R. Chaudhary, Mechanism of geopolymerization and factors influencing its development: A review, J. Mater. Sci. 42 (2007) 729–746. doi:10.1007/s10853-006-0401-4.

[6] T. Alomayri, I.M. Low, Synthesis and characterization of mechanical properties in cotton fiber-reinforced geopolymer composites, J. Asian Ceram. Soc. 1 (2013) 30–34. doi:10.1016/j.jascer.2013.01.002.

[7] T. Alomayri, F.U.A. Shaikh, I.M. Low, Characterisation of cotton fibre-reinforced geopolymer composites, Compos. Part B Eng. 50 (2013) 1–6. doi:10.1016/j.compositesb.2013.01.013.

[8] K.L. Pickering, M.G.A. Efendy, T.M. Le, A review of recent developments in natural fibre composites and their mechanical performance, Compos. Part A Appl. Sci. Manuf. 83 (2016) 98–112. doi:10.1016/j.compositesa.2015.08.038.

[9] M. Criado, A. Fernández Jiménez, I. Sobrados, A. Palomo, J. Sanz, Effect of relative humidity on the reaction products of alkali activated fly ash, J. Eur. Ceram. Soc. 32 (2012) 2799–2807. doi:10.1016/j.jeurceramsoc.2011.11.036.

[10] G. Taveri, E. Bernardo, I. Dlouhy, Mechanical Performance of Glass-Based Geopolymer Matrix Composites Reinforced with Cellulose Fibers, Materials (Basel). 11 (2018) 2395. doi:10.3390/ma11122395.

[11] M. Torres-Carrasco, F. Puertas, Waste glass in the geopolymer preparation. Mechanical and microstructural characterisation, J. Clean. Prod. 90 (2015) 397–408. doi:10.1016/j.jclepro.2014.11.074.

[12] L. Bertolla, I. Dlouhý, P. Tatarko, A. Viani, A. Mahajan, Z. Chlup, M.J. Reece, A.R. Boccaccini, Pressureless spark plasma–sintered Bioglass® 45S5 with enhanced mechanical properties and stress–induced new phase formation, J. Eur. Ceram. Soc. 37 (2017) 2727–2736. doi:10.1016/j.jeurceramsoc.2017.02.003.

[13] ASTM International, ASTM D790 - 17 Standard Test Methods for Flexural Properties of

Unreinforced and Reinforced Plastics and Electrical Insulating Materials, ASTM Stand. (2018). https://www.astm.org/Standards/D790.htm (accessed January 8, 2019).

[14] A.R. Boccaccini, H. Kern, I. Dlouhy, Determining the fracture resistance of fibre-reinforced glass matrix composites by means of the chevron-notch flexural technique, Mater. Sci. Eng. A. 308 (2001) 111–117. doi:10.1016/S0921-5093(00)01984-5.

[15] A. Monshi, Quantitative Phase Analysis in Industrial Research, in: ACXRI 1996, 1996: pp. 1–4. doi:10.1007/978-94-007-5580-2.

[16] N. Gamage, K. Liyanage, S. Fragomeni, S. Setunge, Overview of different types of fly ash and their use as a building and construction material, in: Int. Conf. Struct. Eng. Constr. Manag., 2013. http://dl.lib.mrt.ac.lk/handle/123/9367.

[17] R.C. Joshi, R.P. Lohtia, Types and Properties of Fly Ash, Prog. Cem. Concr. (1985) 118–157.

[18] R.P. Williams, A. Van Riessen, Determination of the reactive component of fly ashes for geopolymer production using XRF and XRD, Fuel. 89 (2010) 3683–3692. doi:10.1016/j.fuel.2010.07.031.

[19] M. Sitarz, W. Mozgawa, M. Handke, Rings in the structure of silicate glasses, J. Mol. Struct. 511–512 (1999) 281–285. doi:10.1016/S0022-2860(99)00169-6.

[20] I. Lecomte, C. Henrist, M. Liégeois, F. Maseri, A. Rulmont, R. Cloots, (Micro)-structural comparison between geopolymers, alkali-activated slag cement and Portland cement, J. Eur. Ceram. Soc. 26 (2006) 3789–3797. doi:10.1016/j.jeurceramsoc.2005.12.021.

[21] J.W. Phair, J.S.J. Van Deventer, Effect of the silicate activator pH on the microstructural characteristics of waste-based geopolymers, Int. J. Miner. Process. 66 (2002) 121–143. doi:http://dx.doi.org/10.1016/S0301-7516(02)00013-3.

[22] E. Arioz, Ö. Arioz, Ö.M. Koç, The Effect of Curing Conditions on the Properties of Geopolymer Samples, Int. J. Chem. Eng. Appl. 4 (2013) 4–7. doi:10.7763/IJCEA.2013.V4.339.

[23] M. Criado, A. Fernández-Jiménez, A. Palomo, Alkali activation of fly ash: Effect of the SiO2/Na2O ratio. Part I: FTIR study, Microporous Mesoporous Mater. 106 (2007) 180–191. doi:10.1016/j.micromeso.2007.02.055.

[24] S.M. Bobrowski A., Stypula B., Hutera B., Drozynski D., Ftir Spectroscopy of Water Glass - The Binder Moulding Modified by ZnO Nanoparticles, 51 (2012) 477–480.

[25] G.Taveri, S.Grasso, Bio-Inspired Hydro-Pressure Consolidation of Silica, Adv. Funct. Mater. 1805794 (2018) 1–22. doi:10.1002/adfm.201805794.

[26] S.A. Bernal, J.L. Provis, V. Rose, R. Mejía De Gutierrez, Evolution of binder structure in sodium silicate-activated slag-metakaolin blends, Cem. Concr. Compos. 33 (2011) 46–54. doi:10.1016/j.cemconcomp.2010.09.004.

[27] J.E. Oh, Y. Jun, Y. Jeong, P.J.M. Monteiro, The importance of the network-modifying element content in fly ash as a simple measure to predict its strength potential for alkali-activation, Cem. Concr. Compos. 57 (2014) 44–54. doi:10.1016/j.cemconcomp.2014.12.001.

[28] L. van Wullen, W. Muller-Warmuth, 11B MAS NMR spectroscopy for characterizing the structure of glasses, Solid State Nucl. Magn. Reson. 2 (1993) 279–284. doi:10.1016/0926-2040(93)90009-C.

[29] C. Nicholson, B. Murray, R.A. Fletcher, D.R.M. Brew, K.J.D. MacKenzie, M. Schmuker, Novel geopolymer materials containing borate structural units, in: Geopolymergreen Chem. Sustain. Dev. Solut., Saint-Quentin (France), 2005.

[30] A. Grandjean, M. Malki, V. Montouillout, F. Debruycker, D. Massiot, Electrical conductivity and 11B NMR studies of sodium borosilicate glasses, J. Non. Cryst. Solids. 354 (2008) 1664–1670. doi:10.1016/j.jnoncrysol.2007.10.007.

[31] S. Sen, Z. Xu, J.. Stebbins, Temperature dependent structural changes in borate, borosilicate and boroaluminate liquids: high-resolution 11B, ^{29}Si and ^{27}Al NMR studies, J. Non. Cryst. Solids. 226 (1998) 29–40. doi:10.1016/S0022-3093(97)00491-2.

[32] M. Criado, A. Fernandez-Jimenez, a G. de la Torre, M. a G. Aranda, A. Palomo, An XRD study of the effect of the SiO2/Na2O ratio on the alkali activation of fly ash, Cem. Concr. Res. 37 (2007) 671–679. doi:10.1016/j.cemconres.2007.01.013.

7. Dissemination related to this work

International conferences

- "Mechanical characterization of fly-ash/borosilicate based geopolymers". World of Coal Ash Conference (WOCA), May 9th – 11th 2017, Lexington (USA). Oral presentation.
- "Properties of geopolymers incorporating wastes". 12th Pacific Rim conference (PACRIM), May 21st – 27th 2017, Waikoloa, Hawaii (USA). Oral presentation.
- "The importance to use borosilicate in geopolymers incorporating wastes". 15th Conference & Exhibition of the European Ceramics Society, July 9th – 13th 2017, Budapest (H). Oral presentation.
- "Geopolymer incorporating wastes and composites processing". 12th International Conference on Ceramic Materials and Components for Energy Environmental Applications (CMCEE18), July 22nd – 27th 2018, Singapore. Oral Presentation.
- "Mechanical and Fracture Performance of Cellulose Fibers Based Geopolymeric Composites Incorporating Wastes". Technical Meeting and Exhibition on Materials Science & Technology (MS&T18), October 14th – 18th 2018, Columbus, Ohio (USA). Oral Presentation.

Publications

- **G. Taveri**, J. Tousek, E. Bernardo, N. Toniolo, A.R. Boccaccini, I. Dlouhy, Proving the role of boron in the structure of fly-ash / borosilicate glass based geopolymers, Mater. Lett. 200 (2017) 105–108. doi:10.1016/j.matlet.2017.04.107 (**Impact factor**: 2.687).
- N. Toniolo, **G. Taveri**, K. Hurle, J.A. Roether, P. Ercole, I. Dlouhy, A.R. Boccaccini, Fly-Ash-Based Geopolymers: How the Addition of Recycled Glass or Red Mud Waste Influences the Structural and Mechanical Properties, J. Ceram. Sci. Technol., 08 [3] 411-420 (2017). doi: 10.4416/JCST2017-00053 (**Impact factor**: 1.220).
- **G. Taveri**, S. Grasso, F. Gucci, J. Tousek and I. Dlouhy, Bio-Inspired Hydro-Pressure Consolidation of Silica, Adv. Func. Mat. 2018, 1805794. DOI: 10.1002/adfm.201805794 (**Impact factor**: 13.325).
- **G. Taveri**, E. Bernardo and I. Dlouhy, Mechanical Performance of Glass-Based Geopolymer Matrix Composites Reinforced with Cellulose Fibers, Materials 2018, 11, 2395. DOI: 10.3390/ma11122395 (**Impact factor**: 2.467).
- A. Rincon Romero, S. Tamburini, **G. Taveri**, J. Tousek, I. Dlouhy and E. Bernardo, Extension of the 'Inorganic Gel Casting' Process to the Manufacturing of Boro-Alumino-Silicate Glass Foams, Materials 2018, 11, 2545. DOI: 10.3390/ma11122545 (**Impact factor**: 2.467).
- Czech patent application Nr. D18079023, file Nr. PV 2018-420, Inventor: **G. Taveri**, co-authors: S. Grasso, I. Dlouhy. Title: Proces zhutňování anorganických prášků za působení hydrostatického tlaku a zařízení k tomuto.